



ACADÉMIE
DES SCIENCES
INSTITUT DE FRANCE

Comptes Rendus

Chimie


Luce Janice Ndzimbou, Rayan Chkair, Gautier Mark Arthur Ndong
Ntoutoume, Mona Diab-Assaf, Guillaume Chemin, Bertrand Liagre,
Frédérique Brégier and Vincent Sol

**Synthesis of long-wavelength-absorbing photosensitizer/nanoparticle conjugates
and their in vitro PDT evaluation on colorectal cancer cell lines**

Volume 28 (2025), p. 215-224

Online since: 5 March 2025

<https://doi.org/10.5802/crchim.383>

 This article is licensed under the
CREATIVE COMMONS ATTRIBUTION 4.0 INTERNATIONAL LICENSE.
<http://creativecommons.org/licenses/by/4.0/>



The Comptes Rendus. Chimie are a member of the
Mersenne Center for open scientific publishing
www.centre-mersenne.org — e-ISSN : 1878-1543



Research article

Synthesis of long-wavelength-absorbing photosensitizer/nanoparticle conjugates and their in vitro PDT evaluation on colorectal cancer cell lines

Luce Janice Ndzimbou^{Ⓢ, a}, Rayan Chkair^{Ⓢ, a}, Gautier Mark Arthur Ndong Ntoutoume^a, Mona Diab-Assaf^b, Guillaume Chemin^{Ⓢ, a}, Bertrand Liagre^{Ⓢ, a}, Frédérique Brégier^{Ⓢ, a} and Vincent Sol^{Ⓢ, *, a}

^a Univ. Limoges, LABCiS, UR 22722, F-87000 Limoges, France

^b Doctoral School of Sciences and Technology, Lebanese University, Hadath El Jebbeh, Beyrouth 21219, Lebanon

E-mail: vincent.sol@unilim.fr (V. Sol)

Abstract. Starting from purpurin-18, a stable purpurin-18 imide derivative with intensive absorption in the near infrared has been synthesized. The opening of the exocycle anhydride by a primary alkylamine bearing an adamantyl group, allows after cyclization the formation of an imide function. This reaction led to the purpurinimide adamantane derivative (PIA) which enables the inclusion of a photosensitizer in the cavity of cationic cyclodextrin coupled to cellulose nanocrystals (CNCs/ β -CD⁺). Preliminary in vitro results showed that CNCs/ β -CD⁺ complexes improved internalization of photosensitizers into HCT116 and HT-29 colorectal cancer cell lines. Moreover, MTT (3-[4,5-dimethylthiazol-2-yl]-2,5 diphenyl tetrazolium bromide) assay of CNCs/ β -CD⁺/PIA complexes showed significant dose-dependent phototoxicity after illumination with red light, with IC₅₀ values of 2.5 and 8.7 nM, for HT 116 and HT-29, respectively, and very low dark toxicity. The current results suggest that these nanoparticle/photosensitizer complexes are promising and useful tools for photodynamic therapy (PDT).

Keywords. Purpurinimide, Photosensitizers, Cellulose nanocrystals, Photodynamic therapy (PDT), Colorectal cancer.

Funding. Campus France, Agence Nationale des Bourses du Gabon, Ligue Nationale contre le Cancer (CD 87 and CD 23), Conseil Régional de Nouvelle Aquitaine.

Manuscript received 9 August 2024, revised 15 January 2025, accepted 5 February 2025.

1. Introduction

Colorectal cancer is the second most deadly cancer, accounting for 9.4% of the nearly 10 million worldwide cancer deaths in 2020 [1], and it remains a major public health problem. Surgery is generally the main option for treating colorectal cancer, often preceded and/or followed by chemotherapy or radiotherapy. These traditional therapies are often accompanied by myelosuppression, multidrug

resistance, and numerous side effects linked to damages to healthy cells. Today photodynamic therapy (PDT) is a promising alternative treatment due to a series of advantages such as fewer side effects and toxicity, and PDT does not induce intrinsic or acquired resistance mechanisms [2]. This therapeutic approach requires the presence of molecular oxygen, the use of a photosensitizer (PS), and irradiation with light of appropriate wavelength. Upon irradiation, the PS is excited to a higher-energy state from which, by energy or electron transfer to ground state/air oxygen (³O₂), it generates singlet oxygen (¹O₂) and other reactive oxygen species

* Corresponding author

(ROS) which induce multiple damage to the tumor cell [3,4]. Ideally, PSs should be characterized by a high $^1\text{O}_2$ quantum yield and would not exhibit cytotoxicity in the dark; in addition, they must be able to absorb light in the near-infrared (NIR) spectral region since NIR light within the phototherapeutic window ($\lambda = 650\text{--}850$ nm) can penetrate rather deeply into tissues. Another key point to avoid unwanted side effects is the preferential accumulation of PS in tumors [5,6]. Thus, one approach to target solid tumors is to exploit the enhanced permeability and retention (EPR) effect [7]. Over the past decade a large number of nanoparticle-based PS delivery systems have been developed [8,9]. These nanocarriers include silica-[10], gold-[11], and natural polymer-based nanoparticles [12]. Polysaccharides have been widely explored for the design and development of nanocarriers due to their numerous advantages, including high water solubility, good biocompatibility, low toxicity, biodegradability and abundance of sources. We have recently reported the synthesis of nanoparticles consisting of covalently bonded porphyrins[13] or pheophorbide *a* to modified xylan [14]. These nanoparticles exhibited a dose-dependent phototoxicity only when irradiated with red light but their aggregation tendency, leading to a reduction in photodynamic efficiency, is a major drawback. To overcome this issue, nanoconjugates consisting of negatively charged cellulose nanocrystals (CNCs) and cationic β -cyclodextrin were developed to encapsulate protoporphyrin IX derivatives bearing an adamantane group [15]. The *in vitro* evaluation of this nanoparticle-based PS against HT-29 colorectal cancer cells showed a clear increase in efficacy compared with the free PS. This nanoparticle form appears to be a very promising tool for the vectorization of PSs. Purpunin-18 (Pp-18) possesses a strong absorption band in the red region (702 nm in CHCl_3), making it a potential PS for PDT, as red light penetrates deeply into animal tissues [16]. Unfortunately, direct use of Pp-18 as PS is limited, due to the presence of a cyclic anhydride, which readily opens after alkaline treatment or in biological media to form chlorin *p6* with a hypsochromic shift of the Q absorption band around 662–665 nm [17–19]. In addition, the high hydrophobicity of Pp-18 leads to its aggregation at physiological pH and reduces its bioavailability [20,21]. To overcome these issues, it has been shown that it is possible to gen-

erate more stable PSs such as purpurinimides with a bathochromic red-shift and excellent *in vitro* and *in vivo* PDT efficacy [22,23]. CNCs were obtained by sulfuric acid hydrolysis of microcrystalline cellulose, which removed amorphous regions and introduced negatively charged sulfate groups that cause electrostatic repulsion forces between suspended particles [24,25]. These negative charges promote the addition, via electrostatic coupling, of positively charged β -Cyclodextrin ($\beta\text{-CD}^+$) previously functionalized with glycidyltrimethyl ammonium chloride (GTAC) [26].

In this work, to obtain a more stable purpurinimide PS than Pp-18 with red-shift light absorption, we transformed the Pp-18 anhydride ring into a cyclic imide to which an adamantyl group is attached. Indeed the adamantyl moiety, which is a spherical entity with a diameter of 6.5 Å, perfectly fits into the cavity diameter of $\beta\text{-CD}$ (6.0–7.0 Å) [27]. Moreover, $\beta\text{-CD}$ /adamantane complexes have found several important applications in supramolecular chemistry and biomedical applications due to their high stability [28]. In a second step, a complex between the newly synthesized PS and cellulose-cyclodextrin nanoparticles was formed. Finally, using PDT, the antiproliferative activity of this conjugate against HCT116 and HT-29 colorectal cancer cell lines was tested [27].

2. Results and discussion

2.1. Synthesis and characterization of the purpurinimide adamantane derivative (PIA)

The hemisynthesis of Pp-18 from chlorophyll *a* was first performed following a previously reported procedure [29]. Pp-18 was reacted with *N*-(2-aminoethyl)adamantyl-1-carboxamide hydrochloride in the presence of diisopropylamine (DIPEA) to produce a mixture of two chlorin-*p6* derivatives (not isolated) via the opening of the Pp-18 anhydride exocycle. After solvent evaporation and treatment of the crude reaction mixture with acetic anhydride, an intramolecular cyclization of the two chlorin *p6* derivatives took place. After purification by preparative thin layer chromatography, the purpurinimide adamantane derivative (PIA) was obtained in 32% yield (Scheme 1). The chemical structure of PIA

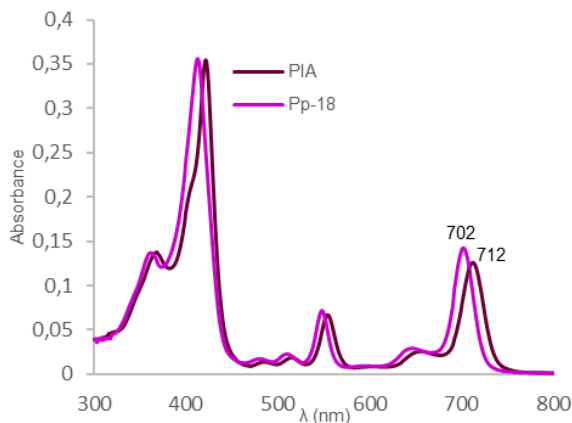


Figure 1. UV-Visible absorption spectra of Pp-18 and PIA in CHCl_3 .

was established by IR, ^1H , ^{13}C NMR and HRMS (Figures S5–S10).

UV-Visible monitoring of the reaction showed that conversion of the anhydride of purpurin-18 to the cyclic imide of PIA was accompanied by a shift in the absorption maximum from 702 to 712 nm in CHCl_3 (Figure 1).

2.2. Synthesis and characterization of cellulose nanocrystals/cationic β -cyclodextrin/purpurinimide adamantane derivative (CNCs/ β -CD $^+$ /PIA) complexes

After sulfuric acid hydrolysis of microcrystalline cellulose, cellulose nanocrystals (CNCs) were obtained in 29% yield according to previously described methods (Scheme 2a) [24,25]. The high zeta potential value of -51.8 ± 1.5 mV exhibited by CNCs (at 1.52/1000 w/w, Figure S1a) confirmed the presence of negatively charged sulfate groups on the surface of CNCs [24,30]. This absolute value, higher than 30 mV, indicated a high degree of stability of the CNCs in aqueous suspension [31,32]. FTIR spectra of CNCs showed peaks at 1205 cm^{-1} and 817 cm^{-1} that were assigned to sulfate esters groups on the CNCs surface, resulting from hydrolysis with sulfuric acid [33,34] (Figure S10). In parallel, positive charges were introduced on β -cyclodextrin by functionalization with a large excess of glycidyltrimethylammonium chloride (GTAC) in alkaline aqueous medium (Scheme 2b) according to Chisholm and Wenzel [35].

Characterization of the final product is in agreement with the literature data (Figures S2 and S3) [26,35]. Finally, mixing β -CD $^+$ with CNCs resulted in the formation of CNCs/ β -CD $^+$ complexes via electrostatic interactions (Scheme 2) [26]. These complexes were then separated from free β -CD $^+$ by centrifugation for 10 min at 13,000 rpm. To see how the characteristics have evolved after coupling, zeta potential measurements were conducted on CNCs/ β -CD $^+$ without dilution to determine their overall surface charge; their hydrodynamic size was measured on a 21-fold dilution (Table 1, Figure S1b). A significant increase in zeta potential from -51.8 ± 1.5 mV for CNCs to 29.77 ± 2.67 mV for CNCs/ β -CD $^+$ was observed (Table 1). The latter value, close to 30 mV, indicated that the dispersion was stable [32]. Analyzed by dynamic light scattering (DLS), this suspension showed an apparent hydrodynamic particle size of 438.97 ± 13 nm compared to 165.5 ± 2.1 nm for CNCs (Figure S1, Table 1). The FTIR spectrum of CNCs/ β -CD $^+$ differs from that of CNCs, with the appearance of a new peak at 1478 cm^{-1} attributed to the $-\text{N}^+-\text{CH}_3$ group of β -CD $^+$, indicating the presence of β -CD $^+$ on the CNCs surface (FTIR spectrum of CNCs/ β -CD $^+$ /PIA, Figure S10). These data are a good indication that positively charged β -CD $^+$ was successfully complexed with CNCs. PIA was loaded into the cavity of the complexed β -CD $^+$ (Scheme 2c) thanks to the hydrophobic nature of the adamantane group. Briefly, a solution of PIA in acetone was mixed with aqueous CNCs/ β -CD $^+$ under ultrasound and magnetic stirring. At the end of the reaction, complexes were purified by centrifugation for 10 min at 10,000 rpm. A decrease in zeta potential from 29.77 ± 2.67 mV for CNCs/ β -CD $^+$ to 19.97 ± 0.15 mV for CNCs/ β -CD $^+$ /PIA was observed (Table 1). This slight decrease could be explained by the carboxylate group of PIA. The new value around 20 mV indicated that the dispersion was relatively to moderately stable [32]. The successful inclusion of PIA in complexes was also confirmed by FT-IR spectroscopy (Figure S10) with peaks at 1724 cm^{-1} , 1679 cm^{-1} , 1641 cm^{-1} , 1600 cm^{-1} , due to, respectively, vibrations of C=O, C=O (amide bond), N-H (amide function), C=C. The concentration of PIA in CNCs/ β -CD $^+$ complexes was determined by UV-Vis spectroscopy around 3.65×10^{-4} mol/L.

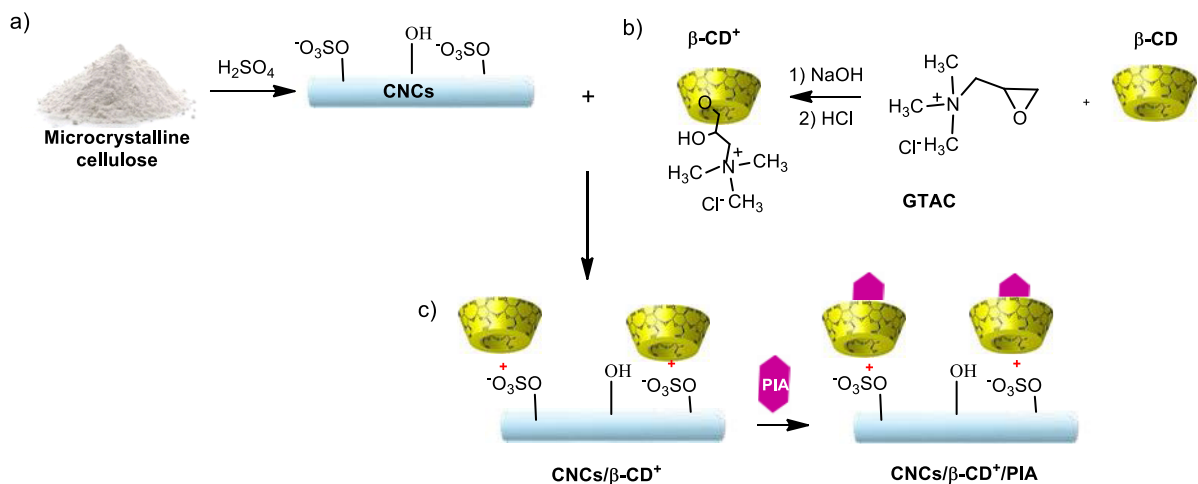
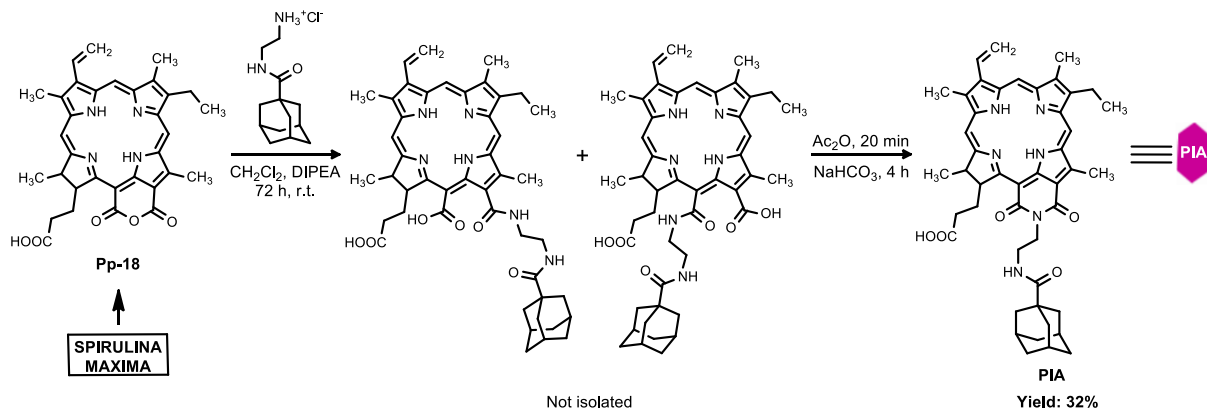


Table 1. Size distribution, PDI and zeta potential (ζ) of CNCs, CNCs/ β -CD⁺ and CNCs/ β -CD⁺/PIA

	CNCs	CNCs/ β -CD ⁺	CNCs/ β -CD ⁺ /PIA
Size (nm)	165.5 \pm 2.1	438.97 \pm 13	-
PDI	0.296	0.196	-
ζ (mV)	-51.8 \pm 1.5	29.77 \pm 2.67	19.97 \pm 0.15

2.3. *In vitro* biological studies

Uptake of PIA and CNCs/ β -CD⁺/PIA complexes by HCT116 and HT-29 cells was studied by fluorescence confocal microscopy (Figure 2).

Cellular accumulation was observed after 24 h incubation with PIA and CNCs/ β -CD⁺/PIA. Incubations in presence of CNCs/ β -CD⁺/PIA led to an increased accumulation of PSs, regardless of the cell line. These results demonstrate the important role

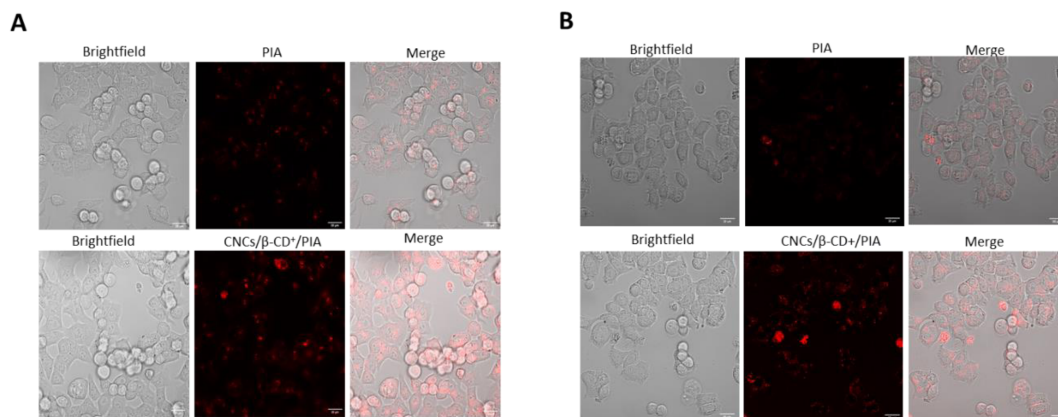


Figure 2. Cellular internalization of PIA and CNCs/ β -CD⁺/PIA in human colorectal cancer cell lines HCT116 (A) and HT-29 (B). Cells were grown for 24 h in chamber slides coated with type I collagen and acetic acid. Cells were then treated with PS at IC₅₀ values. After 24 h, the red fluorescence of PS was assessed by confocal microscopy. ImageJ software (version 1.52p) was used to determine colocalization. White scale bar = 20 μ m.

played by CNCs/ β -CD⁺ in the cellular uptake of the PS and are in agreement with our previous results [26]. Photodynamic activities of PIA alone or CNCs/ β -CD⁺/PIA complexes were evaluated in HCT116 and HT-29 colorectal cancer cell lines using MTT (3-[4,5-dimethylthiazol-2-yl]-2,5 diphenyl tetrazolium bromide) assays (Figure 3). The cancer cell lines were incubated with different concentrations of CNCs/ β -CD⁺/PIA complexes as aqueous solution or PIA alone in DMSO at 0.13, 1.3, 6.5, 13, 26 and 39 nM for 24 h. Cells were then illuminated for 7 min at 650 nm (light dose 30 J/cm²) and then incubated in the dark for 24 and 48 h. Within the concentration range tested, we observed a low cytotoxicity in the dark. Under irradiation, the cytotoxicities of PIA alone or CNCs/ β -CD⁺/PIA were much stronger in comparison with the control tests in the dark.

CNCs/ β -CD⁺ complexes alone were shown to only slightly reduce cancer cell proliferation after 48 h [26]; therefore it can be concluded that the antiproliferative efficacy observed in these experiments, on the two cancer cell lines, is mainly due to the presence of PIA in the CNCs/ β -CD⁺. In both cases, whether PIA is alone or complexed, the IC₅₀ values after 48 h are only slightly lower than those obtained after 24 h (Table 2).

As shown in Figure 3, a dose-dependent antiproliferative effect was observed in both colon cancer

cell lines but HT-29 cells were more resistant than HCT116, as previously observed during in vitro assay using both cell lines [36,37]. After 48 h photoirradiation, IC₅₀ values of 2 and 3.1 nM were determined for HCT116 and HT-29, respectively. Encapsulation into CNCs/ β -CD⁺ appeared to slightly decrease the toxicity of PIA. However, the IC₅₀ values remained in the nanomolar range, with IC₅₀ values of 2.5 and 8.7 nM against HCT116 and HT-29, respectively. The IC₅₀ values for the CNCs/ β -CD⁺/PIA complex of 13.3 and 46.2 μ g/mL against HCT116 and HT-29, respectively, are relatively low in comparison with a biotoxicity value of 250 μ g/mL reported in the literature [38]. Encapsulation of PIA in complexes proves to be a relevant choice to solubilize PIA in aqueous media and will facilitate its selective accumulation in the tumor tissues via enhanced permeation and retention (EPR) effect. In comparison with previous work, CNCs/ β -CD⁺/PIA showed stronger photocytotoxicities than two different protoporphyrin IX (PpIX) adamantane derivatives also encapsulated into CNCs/ β -CD⁺ (IC₅₀ values of 1000 nM and 420 nM) [15]. PIA and its nanoformulation exhibited excellent PDT efficacies against cancer cell lines.

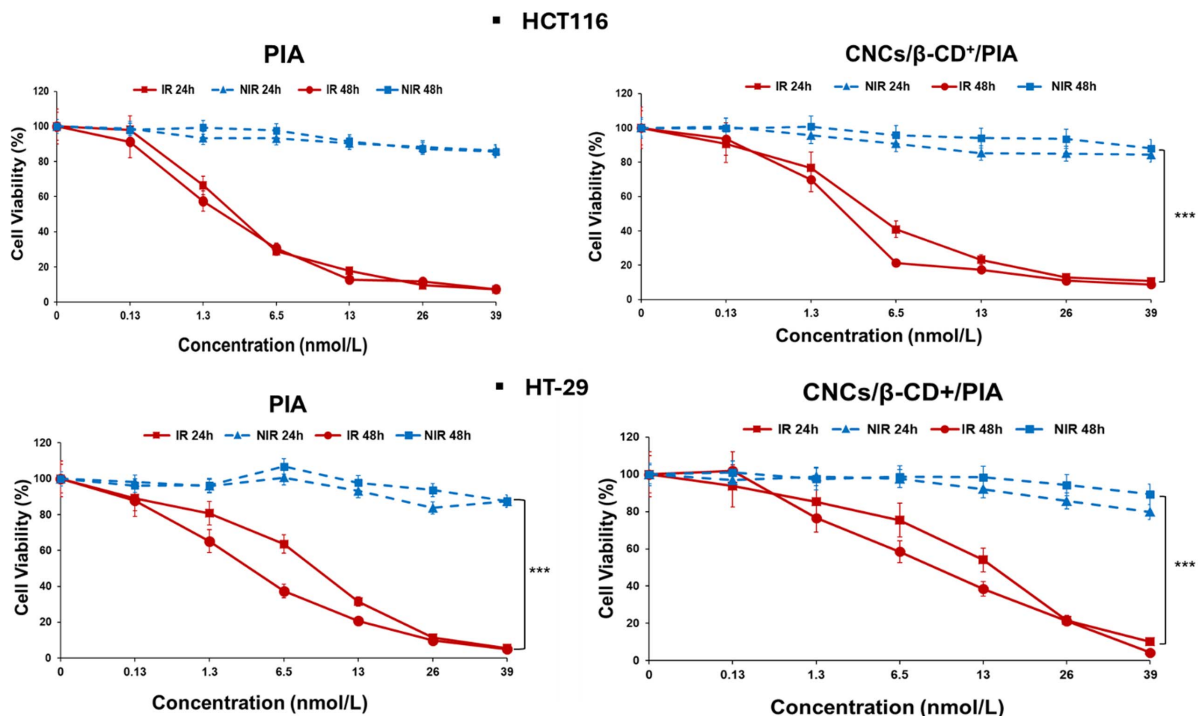


Figure 3. Cell viability in HCT116 and HT-29 colorectal cancer cells as an index of photocytotoxicity (IR) (light, total light dose 30 J/cm^{-2} ; irradiation 7 min, $\lambda = 650 \text{ nm}$) and dark cytotoxicity (NIR) after 24 h incubation times of PIA alone or CNCs/ β -CD $^{+}$ /PIA complexes at concentrations of 0.13 to 39 nM. The percentage of cell viability was determined by MTT (3-(4,5-dimethylthiazol-2-yl)-2,5-diphenyltetrazolium bromide) assay, 24 and 48 h after irradiation. Error bars represent the standard deviation of three replicate experiments. ($h\nu$ = irradiated and no $h\nu$ = non irradiated). Data are represented as mean \pm SEM ($n = 3$). *** $p < 0.001$ relative to the no $h\nu$ at 48 h.

3. Conclusion

In this work, the synthesis of a new purpurin-18 imide derivative bearing an adamantane moiety and the preparation of biocompatible CNCs/ β -CD $^{+}$ /PIA complexes for PDT anticancer therapy were described. ^1H NMR, HRMS, UV-Visible and FTIR spectroscopies indicated that the purpurin-18 imide derivative and its inclusion complexes were successfully obtained. The biological tests demonstrated for the resulting complexes a very good solubility in aqueous media, an increased uptake of hydrophobic PS by cancer cells, and excellent photodynamic efficacy ($\text{IC}_{50} = 2.5$ and 8.7 nM against HCT116 and HT-29 cell lines respectively, 48 h after irradiation). Based on these results, we can suggest that PIA-loaded CNCs/ β -CD $^{+}$ is a promising tool for PDT anticancer therapy.

4. Materials and methods

4.1. Materials

For a list of materials, see Supplementary Information (SI).

4.2. Methods

4.2.1. Synthesis of $13^1,15^1\text{-N-(2-[(1-Adamantylcarbonyl)amino]ethylcycloimide) chlorin p6}$ (purpurinimide adamantane derivative or PIA) (Figure 4)

Purpurin-18 (90.8 mg, 0.1608 mmol, 1 equiv) and N -(2-aminoethyl)adamantyl-1-carboxamide hydrochloride (99.8 mg, 0.3856 mmol, 2.4 equiv) were dissolved in CH_2Cl_2 (10 mL) under argon atmosphere. DIPEA (100 μL , 0.5730 mmol, 3.6 equiv)

Table 2. IC₅₀ values of PIA and CNCs/β-CD⁺/PIA obtained using MTT assay

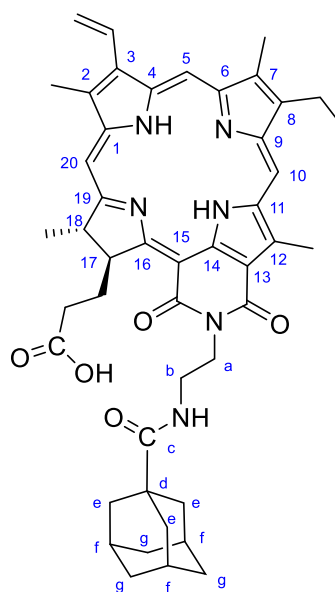
Cell Line	HCT116				<i>P</i> value (48 h relative to 24 h)	HT-29				<i>P</i> value (48 h relative to 24 h)
	24 h		48 h			24 h		48 h		
Incubation time after irradiation (h)	IC ₅₀ ^a	IC ₅₀ ^b	IC ₅₀ ^a	IC ₅₀ ^b		IC ₅₀ ^a	IC ₅₀ ^b	IC ₅₀ ^a	IC ₅₀ ^b	
PIA	2.6	-	2	-	0.3118 (NS)	8.7	-	3.1	-	0.0458 (*)
CNCs/β-CD ⁺ /PIA	4.3	22.9	2.5	13.3	0.0856 (NS)	10	53.2	8.7	46.2	0.0565 (NS)
<i>P</i> value (PIA relative to CNCs/β-CD ⁺ /PIA)	0.0306 (*)	-	0.0876 (NS)	-	-	0.0226 (*)	-	0.0054 (**)	-	-

*Data are expressed as mean ± standard error of the mean (SEM) of three experiments. The statistical significance of results was evaluated using GraphPad Prism 5.0 by a two-tailed unpaired Student's *t*-test, as **p* < 0.05 was considered statistically significant. **p* < 0.05, ***p* < 0.01 *NS: not significant.

^a nmol PIA/L. ^b μg CNCs/β-CD⁺/PIA/mL.

was added and the resulting solution was stirred for 72 h at room temperature; the color of the solution changed from purple to green indicating the formation of the chlorin p6 derivative. CH₂Cl₂ was evaporated and the residue was dissolved in Ac₂O (3 mL) and stirred for 20 min; the color changed from green to purple indicating the formation of the new imide cycle. The resulting mixture was diluted with 5% aqueous NaHCO₃ (90 mL) and stirred for 4 h. The product was extracted with CH₂Cl₂, washed with deionized H₂O, and dried over MgSO₄. After evaporation, the purpurinimide was isolated by preparative thin layer chromatography using CHCl₃/MeOH (95:5) as the eluent and crystallized from CH₂Cl₂/petroleum ether/cyclohexane, yielding 39.6 mg (32%).

CCM Rf (CHCl₃/MeOH 95:5) = 0.17. FTIR/ATR, ν/cm^{-1} : 3333, 2961, 2904, 2850, 1725, 1679, 1641, 1600, 1524. ¹H NMR (500 MHz, CDCl₃): δ_{H} , ppm 9.54 (s, 1 H, H10), 9.31 (s, 1 H, H5), 8.55 (s, 1 H, H₂O), 7.87 (dd, 1 H, *J* = 17.0 and 11.9 Hz, H3¹-CH), 6.45 (bs, 1 H, NH), 6.28 (d, 1 H, *J* = 17.7 Hz, H3²-CH₂), 6.17 (d, 1 H, *J* = 11.4 Hz, H3²-CH₂), 5.69 (m, 1 H, H17), 4.84 (m, 1 H, a-CH₂), 4.60 (m, 1 H, b-CH₂), 4.48 (d, 1 H, *J* = 13.4 Hz, a-CH₂), 4.32 (m, 1 H, H18), 3.76 (s, 3 H, 12-CH₃), 3.59 (q, 2 H, *J* = 7.3 Hz, 8¹-CH₂), 3.42 (d, 1 H, *J* = 13.1 Hz, b-CH₂), 3.32 (s, 3 H, 2-CH₃), 3.14 (s, 3 H, 7-CH₃), 2.70 (m,

**Figure 4.** Structure and numbering of PIA.

1 H, 17¹-CH₂), 2.15-1.92 (m, 3 H, 17¹-CH₂ and 17²-CH₂), 1.82 (d, 3 H, *J* = 8.0 Hz, 18-CH₃), 1.73 (m, 3 H, f-Ad), 1.66 (t, 3 H, *J* = 7.5 Hz, 8²-CH₃), 1.53-1.38 (m, 12 H, e-Ad et g-Ad), 1.10 and -0.10 (s, 2 H, NH). ¹³C NMR (125 MHz, CDCl₃): δ_{C} , ppm 179.8 (1C, Adamantane C=O), 176.5 (1C, C16), 175.8 (1C, C19),

170.4 (1C, COOH), 167.7 (1C, cycloimide C15'), 164.2 (1C, cycloimide C13'), 155.8 (1C, C6), 149.9 (1C, C9), 145.6 (1C, C8), 143.4 (1C, C1), 139.0 (1C, C12), 137.25 and 137.17 (2C, C3, C14), 136.42 and 136.4 (1C, C7 and C4), 131.5 (2C, C2, C11), 128.6 (1C, C3¹), 123.3 (1C, C3²), 115.1 (1, C13), 107.0 (1C, C10), 102.6 (1C, C5), 97.9 (1C, C15), 94.9 (1C, C20), 53.5 (1C, C17), 50.3 (1C, C18), 40.5 (1C, C-Ad_d), 38.64 (3C, CH₂-Ad), 38.56 (1C, NCH₂CH₂NH), 38.2 (1C, NCH₂CH₂NH), 36.2 (3C, CH₂-Ad), 32.2 (1C, C17²-CH₂), 31.4 (1C, C17¹-CH₂), 27.8 (3C, CH-Ad_f), 23.7 (1C, 18-CH₃), 19.4 (1C, 8-CH₂), 17.4 (1C, 8-CH₃), 12.4 (1C, 12-CH₃), 11.9 (1C, 2-CH₃), 11.1 (1C, 7-CH₃). HRMS *m/z*: [M + H]⁺ calc for C₄₆H₅₃N₆O₅ 769.4072; found 769.4080. UV-Visible in DMSO, λ_{max}/nm (ε, 10⁻³ L·mol⁻¹·cm⁻¹): 420 (78), 512 (6.4), 550 (14), 648 (5), 705 (28). UV-Visible in CHCl₃, λ_{max}/nm (ε, 10⁻³ L·mol⁻¹·cm⁻¹): 421 (120), 515 (6), 554 (23), 656 (8), 712 (44).

4.2.2. Production of cellulose nanocrystals (CNCs)

Microcrystalline cellulose (MCC) was used as starting material to obtain CNCs according to previously reported methods [24,25]. Briefly, MCC (2 g) was mixed with H₂SO₄ (40 mL of 61 wt%) using a magnetic stirrer at 45 °C for 1.5 h. The suspension was diluted with cold distilled water (150 mL, 4 °C) to stop the reaction. Then, CNCs were pelleted by centrifugation for 10 min at 3700 rpm and the supernatant was discarded. The pellets were resuspended in H₂O to eliminate excess acid and impurities and then centrifuged for 10 min at 3700 rpm. The supernatant was discarded. The pellets were resuspended in H₂O and centrifuged for 10 min at 3700 rpm. The supernatant containing the CNCs was dialyzed against distilled H₂O using membrane tubing (6–8 KDa cutoff) for 5–6 days. Dialysis H₂O was changed two or three times each day. After dialysis, the resulting solution was completely dispersed by ultrasonic treatment in an ice bath using a Elmasonic S15 for 15 min to give the desired colloidal suspension. After freeze-drying, the yield was determined as 29% using Equation (1). Hydrodynamic size, polydispersity index, and zeta potential measurements were carried out with a 0.152 wt% suspension.

FTIR/ATR *v*/cm⁻¹: 3337, 2900, 1650, 1425, 1369, 1333, 1317, 1281, 1205, 1161, 1111, 1033, 1057, 898, 817 and 776.

The CNCs yield (%) was calculated according to Equation (1):

$$\text{CNCs yield (\%)} = \frac{M_2 \times V_2}{M_1 \times V_1} \times 100 \quad (1)$$

where *M*₁ is the mass of MCC, *M*₂ the mass of the aliquot of lyophilized CNCs, *V*₁ the total volume of collected supernatant CNCs suspension, and *V*₂ the volume of the aliquot of CNCs suspension to be lyophilized.

4.2.3. Cationic β-cyclodextrin (β-CD⁺) synthesis

Cationic β-cyclodextrin was prepared by reacting the native β-cyclodextrin (β-CD) with glycidyltrimethylammonium chloride (GTAC) [35]. Distilled water (20 mL) and β-CD (3.008 g, 2.65 mmol, 1 equiv) were introduced in a round-bottomed flask (100 mL). The pH was adjusted to 12 with NaOH (2M). Then GTAC (14.5 mL, 108 mmol, 40.8 equiv) was added to the mixture. The reaction mixture was stirred at 50 °C for 5 days. The pH was adjusted to 6 with the addition of HCl (2M) and stirring for 30 min at rt. The reaction mixture was dialyzed against distilled water in a dialysis tubing (MWCO Molecular weight cutoff: 500 Da) for 27 h, distilled H₂O was replaced once. After dialysis, the volume of the colorless liquid was brought up to 250 mL with distilled H₂O. Aliquots of this solution were lyophilized and characterized. Degree of substitution (DS) = 2 was determined by integrating the appropriate signals of the ¹H NMR spectrum.

FTIR/ATR (cm⁻¹): 3345, 2929, 1638, 1478, 1418, 1353, 1148, 1108 and 1024. ¹H NMR (500 MHz, D₂O): δ (ppm) = 5.33 (d, 1 H, *J* = 5.75 Hz), 4.48 (m, 2 H), 4.35–4.26 (m, 1 H), 4.08–3.81 (m, 6 H), 3.78–3.69 (m, 2 H), 3.64 (m, 4 H), 3.6–3.42 (m, 6 H), 3.38–3.33 (m, 2 H) and 3.27 (s, 18 H).

4.2.4. Preparation of CNCs/β-CD⁺

The CNCs/β-CD⁺ complex was prepared as previously described with slight modification [26]. β-CD⁺ (40 mL, 1.42 mg/mL) was added slowly to CNCs (11 mL, 1.42 mg/mL) under ultrasound in an ice bath for 15 min and stirred overnight at rt. The mixture was then centrifuged at 13,000 rpm for 10 min to eliminate free β-CD⁺. The precipitate was dispersed in distilled H₂O (20 mL). The final solution was used to encapsulate PIA.

4.2.5. Preparation of purpurinimide-loaded cellulose nanocrystals/cationic- β -cyclodextrin (CNCs/ β -CD⁺/PIA)

PIA (5 mg) was dissolved in acetone (800 μ L) and introduced into aqueous CNCs/ β -CD⁺ suspension (11 mL) under ultrasound in an ice bath for 5 min. The solution was then protected from light and stirred for 1.25 h in an ice bath. The complex was centrifuged at 10 000 rpm for 10 min to eliminate free PIA remaining in the supernatant. The pellet was redispersed in distilled H₂O (11 mL) to form the final suspension of inclusion complex. Aliquots (0.5 mL) of this final suspension were lyophilized and then solubilized in DMSO to determine the loading amount of PIA in CNCs/ β -CD⁺/PIA, by measurement of absorbance at 420 nm. PIA concentration in CNCs/ β -CD⁺/PIA complex was 3.65×10^{-4} mol/L. To determine the overall surface charge of CNCs/ β -CD⁺/PIA inclusion complex, the zeta potential of the sample was measured without dilution.

FTIR/ATR (cm⁻¹): 3338, 2969, 2904, 2852, 1724, 1679, 1641, 1600, 1526, 1479, 1455, 1426, 1369, 1136, 1315, 1281, 1248, 1205, 1161, 1110, 1056, 1032, 900, 881 and 791.

4.2.6. *In vitro* photoradiation Studies

The two human colorectal cancer cell lines used, HT-29 and HCT116, were provided by the American Type Culture Collection (ATCC-LGC Standards, Mosheim, France). Both cell lines were cultured in RPMI medium supplemented with 10% fetal bovine serum (FBS), L-glutamine (1%), penicillin (100 U/mL), and streptomycin (100 μ g/mL) (all reagents purchased from Gibco BRL, Cergy-Pontoise, France). Cells were cultured in a humidified atmosphere with 5% CO₂ at 37 °C. For all experiments, HCT116 cells were seeded at 1.2×10^4 , and HT-29 cells at 2.1×10^4 cells/cm².

The PDT protocol was performed as follows: 4×10^3 and 7×10^3 cells/well for HCT116 and HT-29, respectively, were seeded into 96-well plates. Cells were grown for 24 h before exposure or not to 0.13, 1.3, 6.5, 13, 26 and 39 nM of PIA in DMSO or CNCs/ β -CD⁺/PIA (aqueous suspension). After 24 h, a red phenol-free medium was added before irradiation or not at 650 nm (30 J/cm²–7 min) delivered from the light source PDT TP-1 (Cosmedico Medizintechnik

GmbH, Schwenningen, Germany). After irradiation, the cells were incubated at 37 °C for 24 and 48 h for further analysis.

Cancer cell viability was assessed by MTT (3-(4,5-dimethylthiazol-2-yl)-2,5-diphenyltetrazolium bromide) method (from Sigma-Aldrich, Saint-Quentin-Fallavier, France). MTT (5 g/L) was added 24 and 48 h after irradiation. After 3 h of incubation, DMSO (100 μ L) was added to each well to dissolve the formazan crystals, and absorbance was recorded at 550 nm using a microplate reader (Thermoscientific MULTISKAN FC). The absorbance *A* values \pm standard deviation was the mean of three experiments. The percent of viability was calculated using Equation (2):

$$\text{Viability (\%)} = \frac{A_{\text{treated}}}{A_{\text{control}}} \times 10 \quad (2)$$

where *A*_{treated} is the absorbance of the treated cells and *A*_{control} the absorbance of the untreated cells.

4.2.7. Cellular internalization by confocal microscopy

To confirm the cellular uptake, HCT116 and HT-29 cells were seeded for 24 h before treatment with PIA or CNCs/ β -CD⁺/PIA complexes at IC₅₀ concentrations in chamber slides (ibidi μ -Slide 8 well from Clinisciences, Martinsried, Germany) coated with a type I collagen (3 mg/mL) and with acetic acid (20 mM) gel. Photos were taken using a confocal microscope (laser Zeiss LSM 510 Meta— \times 1000). Colocalization was assessed using the ImageJ software (version 1.52p).

Declaration of interests

The authors do not work for, advise, own shares in, or receive funds from any organization that could benefit from this article, and have declared no affiliations other than their research organizations.

Acknowledgements

The authors acknowledge logistical and financial support from Campus France, “Agence Nationale des Bourses du Gabon”, “Ligue Nationale contre le Cancer (CD 87 and CD 23)” and “Conseil Régional de Nouvelle Aquitaine”. They wish to thank Dr. Cyril Colas (ICOA-Univ. Orléans) for ESI-HRMS analyses and Dr. Yves Champavier from BISCEM platform for NMR

analysis. They are indebted to Dr. Michel Guilloton for his help in manuscript editing.

Supplementary data

Supporting information for this article is available on the journal's website under <https://doi.org/10.5802/crchim.383> or from the author.

References

- [1] Y. Xi and P. Xu, *Transl. Oncol.* **14** (2021), article no. 101174.
- [2] J. A. Rodrigues and J. H. Correia, *Int. J. Mol. Sci.* **24** (2023), article no. 12204.
- [3] H. I. Pass, *JNCI J. Natl. Cancer Inst.* **85** (1993), pp. 443–456.
- [4] T. J. Dougherty, C. J. Gomer, B. W. Henderson, G. Jori, D. Kessel, M. Korbelik, J. Moan and Q. Peng, *J. Natl. Cancer Inst.* **90** (1998), pp. 889–905.
- [5] J. C. S. Simões, S. Sarpaki, P. Papadimitroulas, B. Therrien and G. Loudos, *J. Med. Chem.* **63** (2020), pp. 14119–14150.
- [6] H. Abrahamse and M. R. Hamblin, *Biochem. J.* **473** (2016), pp. 347–364.
- [7] Y. Matsumura and H. Maeda, *Cancer Res.* **46** (1986), pp. 6387–6392.
- [8] A. V. P. Kumar, S. K. Dubey, S. Tiwari, A. Puri, S. Hejmady, B. Gorain and P. Kesharwani, *Int. J. Pharm.* **606** (2021), article no. 120848.
- [9] M. Q. Mesquita, C. J. Dias, S. Gamelas, M. Fardilha, M. G. P. M. S. Neves and M. A. F. Faustino, *An. Acad. Bras. Ciênc.* **90** (2018), pp. 1101–1130.
- [10] P. Couleaud, V. Morosini, C. Frochot, S. Richeter, L. Raehm and J.-O. Durand, *Nanoscale* **2** (2010), pp. 1083–1095.
- [11] P. García Calavia, G. Bruce, L. Pérez-García and D. A. Russell, *Photochem. Photobiol. Sci.* **17** (2018), pp. 1534–1552.
- [12] L. Li and K. M. Huh, *Biomater. Res.* **18** (2014), article no. 19.
- [13] S. Bouramtane, L. Bretin, J. Godard, et al., *C. R. Chim.* **2021** (24), pp. 127–140.
- [14] S. Bouramtane, L. Bretin, A. Pinon, et al., *J. Appl. Polym. Sci.* **138** (202), article no. 50799.
- [15] G. M. A. Ndong Ntoutoume, R. Granet, J.-P. Mbakidi, et al., *Bioorg. Med. Chem. Lett.* **41** (2021), article no. 128024.
- [16] A. R. Morgan, G. M. Garbo, M. Kreimer-Birnbaum, R. W. Keck, K. Chaudhuri and S. H. Selman, *Cancer Res.* **47** (1987), pp. 496–498.
- [17] A. F. Mironov and E. G. Levinson, in *Photodynamic Therapy of Cancer II*, SPIE: Bellingham, 1995, pp. 312–320.
- [18] A. F. Mironov, V. S. Lebedeva, R. I. Yakubovskaya, N. I. Kazachkina and G. I. Fomina, in *Photochemotherapy of Cancer and Other Diseases*, SPIE: Bellingham, 1999, pp. 59–67.
- [19] S. Sharma, A. Dube, B. Bose and P. K. Gupta, *Cancer Chemother. Pharmacol.* **57** (2006), pp. 500–506.
- [20] V. Pavlíčková, J. Škubník, M. Jurásek and S. Rimpelová, *Appl. Sci.* **11** (2021), article no. 2254.
- [21] V. Pavlíčková, S. Rimpelová, M. Jurásek, et al., *Molecules* **24** (2019), article no. 4477.
- [22] B. C. Cui, I. Yoon, J. Z. Li, W. K. Lee and Y. K. Shim, *Int. J. Mol. Sci.* **15** (2014), pp. 8091–8105.
- [23] G. Zheng, W. R. Potter, S. H. Camacho, et al., *J. Med. Chem.* **44** (2001), pp. 1540–1559.
- [24] L. K. Kian, M. Jawaid, H. Ariffin and Z. Karim, *Int. J. Biol. Macromol.* **114** (2018), pp. 54–63.
- [25] A. Hachaichi, B. Kouini, L. K. Kian, M. Asim, H. Fouad, M. Jawaid and M. Sain, *Materials* **14** (2021), article no. 5313.
- [26] G. M. A. Ndong Ntoutoume, R. Granet, J. P. Mbakidi, et al., *Bioorg. Med. Chem. Lett.* **26** (2016), pp. 941–945.
- [27] X. Zhong, C. Hu, X. Yan, X. Liu and D. Zhu, *J. Mol. Liq.* **272** (2018), pp. 209–217.
- [28] D. Granadero, J. Bordello, M. J. Pérez-Alvite, M. Novo and W. Al-Soufi, *Int. J. Mol. Sci.* **11** (2010), pp. 173–188.
- [29] N. Drogat, M. Barrière, R. Granet, V. Sol and P. Krausz, *Dyes Pigments* **88** (2011), pp. 125–127.
- [30] X. M. Dong, J.-F. Revol and D. G. GRAY, *Cellulose* **5** (1998), pp. 19–32.
- [31] Y. Su, L. Gong and D. Chen, *Adv. Mech. Eng.* **8** (2016), article no. 1687814015627978.
- [32] S. Bhattacharjee, *J. Control. Release* **235** (2016), pp. 337–351.
- [33] P. Lu and Y.-L. Hsieh, *Carbohydr. Polym.* **82** (2010), pp. 329–336.
- [34] I. W. Arnata, S. Suprihatin, F. Fahma, N. Richana and T. C. Sunarti, *Cellulose* **27** (2020), pp. 3121–3141.
- [35] C. D. Chisholm and T. J. Wenzel, *Tetrahedron: Asymmetry* **22** (2011), pp. 62–68.
- [36] S. Bouramtane, L. Bretin, A. Pinon, et al., *Carbohydr. Polym.* **213** (2019), pp. 168–175.
- [37] L. Bretin, A. Pinon, S. Bouramtane, et al., *Cancers (Basel)* **11** (2019), article no. 1474.
- [38] Z. Hanif, F. R. Ahmed, S. W. Shin, Y.-K. Kim and S. H. Um, *Colloids Surf. B: Biointerfaces* **119** (2014), pp. 162–165.